Response to reviewers

*We are **grateful and thank** Associate Editor for thorough assessment of our manuscript and for providing us constructive comments and suggestions.*

*In the revised version, **all the comments and suggestions have been taken into account** and changes have been made to improve the presentation.*

We now add point-by-point reply (in italics, in red color fonts) to the comments and suggestions of the Associate Editor and make clear where and what changes have been made in the revised version of the manuscript.

Comment

Technical correction: Thank you for adding the profile in Figure 4e. It is rather small, and the labels (both in the profile and in the main image) are illegible without significant zoom. Please resize the labels in the inset, and the profile labels in the main Fig 4e panel, to ensure they are readable. You could include it below the main panels if this is easier.

***Response:** As suggested by the Associate Editor, we have revised the Figure 4e.*

We have added both the versions of the Figure 4 below to have a comparison:

26 ***Figure 4 (previous version)***

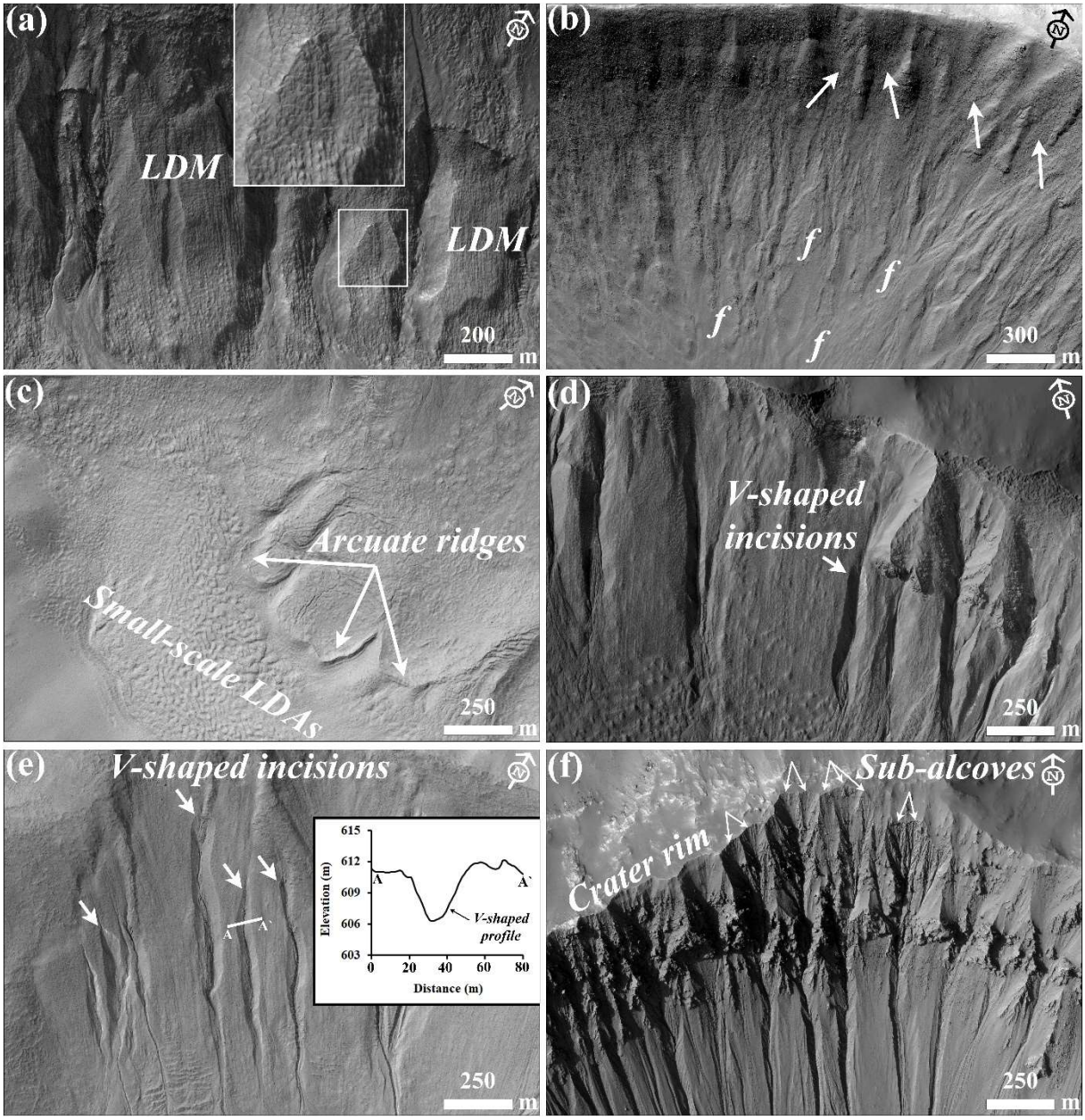

27

28

29

Figure 4 (revised version – this revised Figure 4 has been included in the revised manuscript)

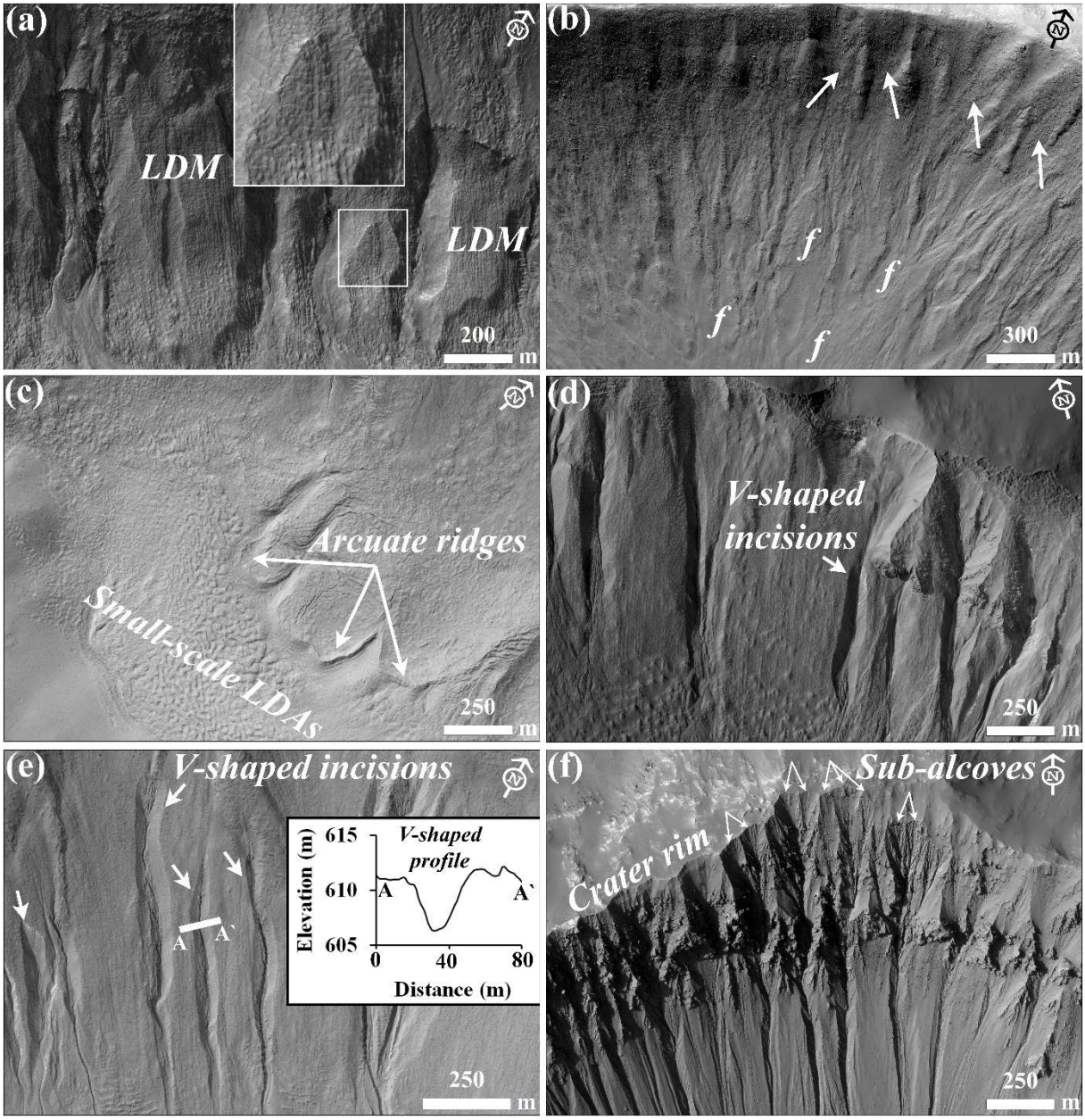

We hope now the labels in the inset, and the profile labels are readable.

Morphologic and Morphometric Differences between Gullies Formed in Different Substrates on Mars: New Insights into the Gully Formation Processes

Rishitosh K. Sinha[1,2], Dwijesh Ray[1], Tjalling De Haas[3], Susan J. Conway[4], Axel Noblet[4]

[1] Physical Research Laboratory, Ahmedabad 380009, Gujarat, India
[2] Indian Institute of Technology, Gandhinagar 382355, Gujarat, India
[3] Faculty of Geoscience, Universiteit Utrecht, Princetonlaan 8a, 3584 CB Utrecht, the Netherlands
[4] Nantes Université, Université d'Angers, Le Mans Université, CNRS UMR 6112 Laboratoire de Planétologie et Géosciences, France

Correspondence to: Rishitosh K. Sinha (rishitosh@prl.res.in)

Abstract. Martian gullies are kilometer-scale geologically young features with a source alcove, transportation channel, and depositional fan. On the walls of impact craters, these gullies typically incise into bedrock or surfaces modified by latitude dependent mantle (LDM; inferred as consisting of ice and admixed dust) and glaciation. To better understand the differences in the alcoves and fans of gullies formed in different substrates and infer the flow types that led to their formation, we have analyzed the morphology and morphometry of 167 gully systems in 29 craters distributed between 30°S and 75°S. Specifically we measured length, width, gradient, area, relief, and relief ratio of the gully alcoves and fans, Melton ratio, relative concavity index, and perimeter, form factor, elongation ratio and circularity ratio of the gully alcoves. Our study reveals that gully alcoves formed in LDM/glacial deposits are more elongated than the gully alcoves formed in bedrock, and possess a distinctive V-shaped cross section. We have found that the mean gradient of fans formed by gullies sourced in bedrock is steeper than the mean gradient of fans of gullies sourced in LDM/glacial deposits. These differences between gullies were found to be statistically significant and discriminant analysis has confirmed that alcove perimeter, alcove relief and fan gradient are the most important variables for differentiating gullies according to their source substrates. The comparison between the Melton ratio, alcove length and fan gradient of Martian and terrestrial gullies reveals that Martian gully systems were likely formed by terrestrial debris-flow like processes. Present-day sublimation of CO_2 ice on Mars may have provided the adequate flow fluidization for the formation of deposits akin to terrestrial debris-flow like deposits.

1 Introduction

Gullies are found on steep slopes polewards of about 30° latitude in both hemispheres on Mars and manifest as kilometer-scale, geologically young features (formed within the last few million years) comprising an alcove, channel, and depositional fan (Malin and Edgett, 2000; Dickson et al., 2007; Reiss et al., 2004; Schon et al., 2009). Gullies occur in a wide assortment of settings, varying from the walls and central peaks of craters to walls of valleys, and steep faces of dunes, hills and polar pits

(e.g. Balme et al., 2006; Dickson et al., 2007; Dickson and Head, 2009; Conway et al., 2011, 2015; Harrison et al., 2015). On the walls of craters, gullies are found to have incised into (1) surfaces covered by latitude dependent mantle (LDM; e.g. Mustard et al., 2001; Dickson et al., 2012, 2015), (2) surfaces modified by former episodes of glaciation (Conway et al., 2018; de Haas 2019a; Sinha and Vijayan, 2017), and (3) bedrock (e.g. Johnsson et al., 2014; de Haas et al., 2019a; Sinha et al., 2020). Detailed investigation of the gullies formed over these different substrates is key to understanding the intricacies of past processes by which these gullies have formed on Mars (Conway et al., 2015; de Haas et al., 2019a).

A variety of models have been proposed to explain the formation of gullies, which include: (1) dry flows triggered by sublimation of CO_2 frost (e.g. Cedillo-Flores et al., 2011; Dundas et al., 2012, 2015; Pilorget and Forget, 2016; de Haas et al., 2019b), (2) debris-flows of an aqueous nature (e.g. Costard et al., 2002; Levy et al., 2010; Conway et al., 2011; Johnsson et al., 2014; de Haas et al., 2019a; Sinha et al., 2020), and (3) fluvial flows (e.g. Heldmann and Mellon, 2004; Heldmann et al., 2005; Dickson et al., 2007; Reiss et al., 2011). To better understand the gully formation processes, morphometric investigation of gullies formed over different substrates needs to be undertaken at a level of detail previously not attempted.

The global distribution of gullies shows a spatial correlation with the landforms indicative of glaciation and LDM deposition on Mars (e.g. Levy et al., 2011; Dickson et al., 2015; Harrison et al., 2015; Conway et al., 2018; de Haas et al., 2019a; Sinha et al., 2020). With respect to glacial landforms, many gullies have formed into viscous flow features (VFFs) and they are found in the same latitude ranges between 30°-60° (e.g. Arfstrom and Hartmann, 2005; de Haas et al., 2019a). VFFs are defined as an umbrella term for glacial-type formations covering a broad range of landforms that include lobate debris aprons (LDAs), concentric crater fills (CCFs), and lineated valley fills (LVFs) (e.g. Squyres, 1978; Levy et al., 2009a; Baker et al., 2010; Hargitai, 2014). Together, they are inferred to be similar to terrestrial debris-covered glaciers (Plaut et al., 2009). With respect to LDM, gullies are mostly found on the pole-facing slopes of crater walls at lower mid-latitudes (30-45°) (e.g. Balme et al. 2006; Kneissl et al. 2010; Harrison et al. 2015; Conway et al. 2017), wherein, LDM is found to be dissected (e.g. Mustard et al., 2001; Milliken et al., 2003; Head et al., 2003). In the higher latitudes (>45°), LDM is found to be continuous (e.g. Kreslavsky and Head, 2000), and gullies are evident at both the pole and equator facing slopes (e.g. Balme et al. 2006; Kneissl et al. 2010; Harrison et al. 2015; Conway et al. 2017). Gullies formed on the formerly glaciated walls of craters are fed from alcoves that do not extend up to the crater rim, and appear elongated to V-shaped, implying gully-channel incision into ice-rich, unlithified sediments (e.g. Aston et al., 2011; de Haas et al., 2019a). The alcoves, channels and fan deposits of gullies formed within craters covered by a smooth drape of LDM, are usually found to have experienced multiple episodes of LDM covering and subsequent reactivation of some of the pre-existing channels or formation of fresh channels within the draped LDM deposits (e.g. Dickson et al., 2015; de Haas et al., 2019a). Additionally, there are gullies that directly emanate from well-defined bedrock alcoves that cut into the crater rim in the absence of LDM and/or glacial deposits (e.g. Johnsson et al., 2014; de Haas et al., 2019a; Sinha et al., 2020). Gullies formed in these craters have alcoves with sharply defined crests and spurs, exposing the underlying bedrock, and meter-sized boulders are found throughout the gully system (e.g. Johnsson et al., 2014;

de Haas et al., 2019a; Sinha et al., 2020). Further, De Haas et al., 2015a found that the stratigraphy of the fans whose source area was in bedrock were more boulder-rich than those fans fed by catchments in LDM. The findings in these studies suggest that a more detailed investigation of the morphology and morphometry of the gullies formed over contrasting substrates is important for improving our understanding of the formative mechanisms of gullies.

In this work, we focus on addressing the following research questions:

(1) Do the morphologies and morphometries of gully systems formed in different substrates differ (i.e. LDM/glacial deposits and bedrock)?

(2) How do the morphometric characteristics of gullies formed on Mars compare to those formed by a range of processes on Earth, and what does that tell us about the formative processes of Martian gullies?

To parameterize the morphometry we will primarily study long profiles. Previously, only a few studies have analyzed the morphometric characteristics of the gullies by studying their long profiles (e.g. Yue et al., 2014; Conway et al., 2015; De Haas et al., 2015a; Hobbs et al., 2015). These studies have focused observations on a part of the gully system and suggested that the differences in the properties of substrate into which the gullies incise play a significant role in promoting the flows that led to gully formation. Hence, for a more detailed differentiation of the gully types and interpretation of the dominant flow type that led to gully formation on Mars, quantification of the morphometric characteristics of the entire gully system is crucial.

2 Study sites and datasets

We characterize the morphologies and morphometries of gullies in 29 craters distributed over the southern hemisphere of Mars between 30° S and 75° S latitude (Fig. 1). These 29 craters are selected based on the availability of publicly released High Resolution Imaging Science Experiment (HiRISE) stereo-pair based digital terrain models (DTMs) or the presence of suitable HiRISE stereo-pair images to produce a DTM ourselves. The HiRISE stereo-pair images are usually ~0.25 - 0.5 m/pixel (McEwen et al., 2007), so the DTM post spacing is ~1-2 m with vertical precision in the range of tens of centimeters (Kirk et al., 2008). Among the 29 gullied craters, publicly released DTMs are available for 25 craters (https://www.uahirise.org/hiwish/maps/dtms.jsp - last accessed 18th September 2021) (Table 1). For the remaining 4 craters, we produced DTMs with the software packages USGS ISIS and BAE Systems SocetSet (Table 1) (Kirk et al., 2008). We investigated HiRISE images of these 29 gullied craters for detailed morphological characterization of the substrate into which the crater wall gullies incise (Table 1).

Table 1. Summary of the craters included in this study, their locations, number of gullies investigated from the crater, substrate on the crater wall in which gullies have incised, key morphological attributes of the substrate, and IDs of HiRISE imagery and DTM used for morphological and morphometric investigation of gullies in these craters.

Crater	Latitude	Longitude	No. of gullies	Substrate	Key morphological attributes	HiRISE ID	HiRISE DTM ID
Artik	34.8° S	131.02° E	2	LDM/glacial deposits	Polygons, V-shaped incisions, arcuate ridges, small-scale LDAs on the floor	ESP_020740_1450	DTEEC_012459_1450_012314_1450_A01
Asimov	47.53° S	4.41° E	4	LDM/glacial deposits	Polygons, V-shaped incisions, mantled alcoves/channels/fans, arcuate ridges, small-scale LDAs inside valleys	ESP_012912_1320	DTEEC_012912_1320_012767_1320_A01
Bunnik	38.07° S	142.07° W	8	LDM/glacial deposits	Polygons, V-shaped incisions, mantled alcoves/channels/fans, arcuate ridges	ESP_047044_1420	DTEEC_002659_1420_002514_1420_U01
Corozal	38.78° S	159.48° E	6	LDM/glacial deposits	Polygons, mantled alcoves/channels/fans, arcuate ridges, small-scale LDAs on the floor	PSP_006261_1410	DTEEC_006261_1410_014093_1410_A01
Dechu	42.23° S	158° W	8	LDM/glacial deposits	Polygons, mantled alcoves/channels/fans, arcuate ridges, small-scale LDAs on the floor	PSP_006866_1375	DTEED_023546_1375_023612_1375_A01
Dunkassa	37.46° S	137.06° W	5	LDM/glacial deposits	Polygons, V-shaped incisions, mantled alcoves/channels/fans, arcuate ridges, small-scale LDAs on the floor	ESP_032011_1425	DTEEC_039488_1420_039343_1420_A01
Hale	35.7° S	36.4° W	8	LDM/glacial deposits	Polygons, V-shaped incisions, mantled alcoves/channels/fans, talus slope deposits	PSP_003209_1445	DTEEC_002932_1445_003209_1445_A01
Langtang	38.13° S	135.95° W	5	LDM/glacial deposits	Polygons, V-shaped incisions, mantled alcoves/channels/fans, arcuate ridges, small-scale LDAs on the floor	ESP_030099_1415	DTEEC_024099_1415_023809_1415_U01

Moni	46.97° S	18.79° E	5	LDM/glacial deposits	Partly infilled alcoves, mantled fan surfaces, arcuate ridges	ESP_056862_1325	DTEEC_007110_1325_006820_1325_A01
Nybyen	37.03° S	16.66° W	8	LDM/glacial deposits	Polygons, mantled alcoves/channels/fans, arcuate ridges	ESP_059448_1425	DTEEC_006663_1425_011436_1425_A01
Palikir	41.56° S	157.87° W	5	LDM/glacial deposits	Polygons, V-shaped incisions, mantled alcoves/channels/fans, arcuate ridges, small-scale LDAs on the floor	ESP_057462_1380	DTEEC_005943_1380_011428_1380_A01
Penticton	38.38° S	96.8° E	7	LDM/glacial deposits	Polygons, V-shaped incisions, mantled alcoves/channels/fans, arcuate ridges, small-scale LDAs on the floor	ESP_029062_1415	DTEEC_001714_1415_001846_1415_U01
Selevac	37.37° S	131.07° W	8	LDM/glacial deposits	Polygons, mantled alcoves/channels/fans, small-scale flows on the floor	ESP_045158_1425	DTEEC_003252_1425_003674_1425_A01
Raga	48.1° S	117.57° W	4	LDM	Polygons, mantled alcoves/channels/fans	ESP_041017_1315	DTEEC_014011_1315_014288_1315_A01
Roseau	41.7° S	150.6° E	1	LDM	Polygons, mantled alcoves/channels/fans	ESP_024115_1380 / ESP_011509_1380	ESP_024115_1380_ESP_011509_1380*
Taltal	39.5° S	125.8° W	7	LDM/glacial deposits	Polygons, V-shaped incisions, mantled alcoves/channels/fans, arcuate ridges, small-scale LDAs on the floor	ESP_037074_1400 / ESP_031259_1400	ESP_037074_1400_ESP_031259_1400*
Talu	40.34° S	20.11° E	7	LDM/glacial deposits	Polygons, V-shaped incisions, mantled alcoves/channels/fans, arcuate ridges, small-scale LDAs on the floor	ESP_011817_1395	DTEEC_011817_1395_011672_1395_O01
Triolet	37.08° S	168.02° W	4	LDM/glacial deposits	Polygons, V-shaped incisions, mantled alcoves/channels/fans, arcuate ridges, small-scale LDAs on the floor	ESP_047190_1425	DTEEC_023586_1425_024008_1425_A01
Unnamed crater	32.31° S	118.55° E	4	LDM/glacial deposits	Polygons, mantled alcoves/channels/fan	PSP_006869_1475	DTEEC_021914_1475_022336_1475_U01

					s, arcuate ridges, small-scale LDAs on the floor		
Unnamed crater in the Argyre basin	40.3° S	40.4° W	6	LDM/glacial deposits	Polygons, mantled alcoves/channels/fans, arcuate ridges, small-scale LDAs on the floor	ESP_032047_1395	DTEEC_012795_1395_013507_1395_A01
Unnamed crater in the Newton basin	38.8° S	156.8° W	5	LDM	Polygons, V-shaped incisions, mantled alcoves/channels/fans	PSP_002686_1410	DTEEC_002620_1410_002686_1410_A01
Unnamed crater north of Corozal crater	38.53° S	159.44° E	5	LDM/glacial deposits	Polygons, mantled alcoves/channels/fans, small-scale LDAs on the floor	ESP_020884_1410	DTEEC_020884_1410_020950_1410_A01
Unnamed crater-1 in the Terra Sirenum	32.55° S	154.11° W	2	LDM	Mantled alcoves/channels/fans	PSP_007380_1470	DTEEC_010597_1470_007380_1470_U01
Unnamed crater-2 in the Terra Sirenum	38.88° S	136.36° W	6	LDM/glacial deposits	Polygons, V-shaped incisions, mantled alcoves/channels/fans, arcuate ridges, small-scale LDAs on the floor	ESP_020407_1410	DTEEC_022108_1410_022385_1410_A01
Istok	45.1° S	85.82° W	8	Bedrock	Alcove cut directly into the original crater-wall material, clasts embedded into fresh deposits on fan	ESP_056668_1345	DTEEC_040607_1345_040251_1345_A01
Galap	37.66° S	167.07° W	8	Bedrock	Alcove cut directly into the original crater-wall material, clasts embedded into fresh deposits on fan	ESP_059770_1420	DTEEC_048983_1420_048693_1420_U01
Gasa	35.73° S	129.4° E	7	Bedrock	Alcove cut directly into the original crater-wall material, clasts embedded into fresh deposits on fan	ESP_057491_1440	DTEEC_021584_1440_022217_1440_A01
Los	35.08° S	76.23° W	7	Bedrock	Alcove cut directly into the original crater-wall material,	ESP_020774_1445 / ESP_050127_1445	ESP_020774_1445_ESP_050127_1445*

					clasts embedded into fresh deposits on fan		
Unnamed crater-3 in the Terra Sirenum	34.27° S	165.71° E	7	Bedrock	Alcove cut directly into the original crater-wall material, clasts embedded into fresh deposits on fan	ESP_049261_1455 / ESP_049828_1455	ESP_049261_1455_ ESP_049828_1455*

129

130 *(*) DTMs are produced with the software packages USGS ISIS and BAE Systems SocetSet.*

131

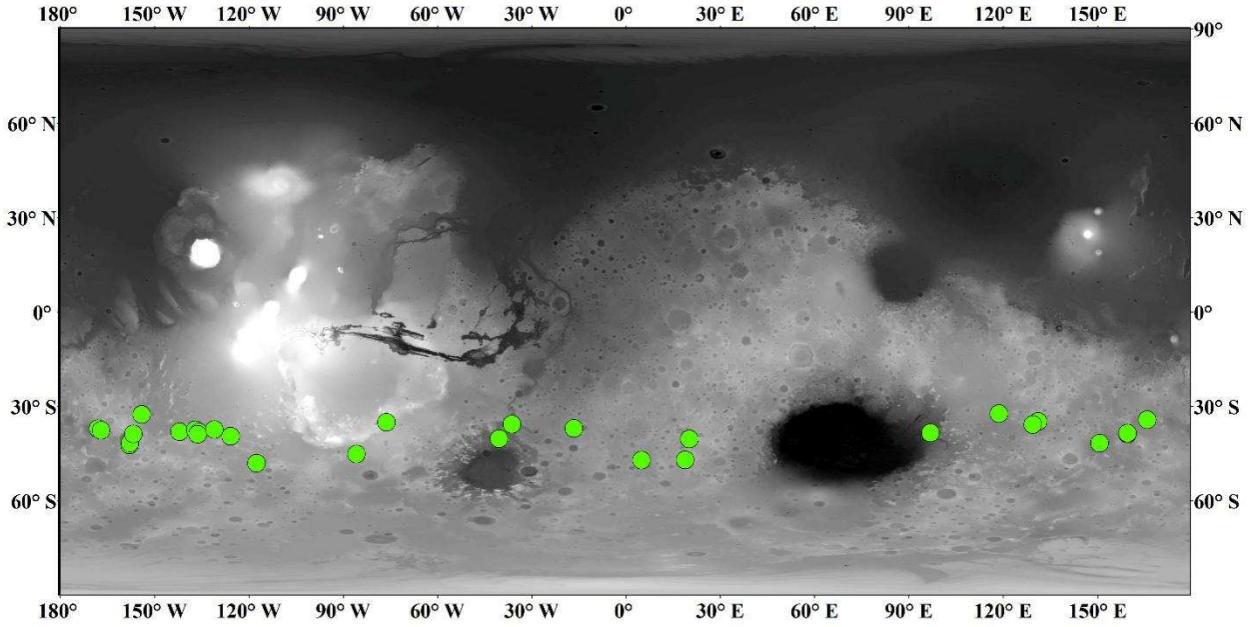

132 **Figure 1: Locations of craters analyzed in this study (green circles). Background: Mars Orbiter Laser Altimeter gridded data, where**
133 **white is high elevation and black is low elevation, credit MOLA Science Team/NASA/JPL.**

134

135 **3 Approach**

136 **3.1 Identification of substrate**

137 The substrate into which the gullies have incised is identified based on the following criteria:

138 1. LDM/glacial deposits: Any crater whose gullies incise walls that appear to be softened by the drape of smooth mantling
139 material with polygonal cracks is inferred to have LDM as the substrate within which gullies have incised (e.g. Mustard et al.,

2001; Kreslavsky and Head, 2002; Levy et al., 2009a; Conway et al., 2018; de Haas et al., 2019a) (Fig. 2a-b). The gully alcoves on the walls of these craters may be partially to completely filled by LDM, and in some cases, polygonized LDM materials may be seen covering the alcove walls (e.g. Christensen, 2003; Conway et al., 2018; de Haas et al., 2019a). These infilled alcoves on the crater walls are not the alcoves of gullies formed within the LDM substrate; instead, they represent the alcoves that were formed prior to the LDM emplacement epoch. Additionally, gullied craters that show evidence in the form of arcuate ridges at the foot of the walls and VFFs that cover part or the entire crater floor are inferred to have been modified by one or multiple episodes of glaciation (e.g. Arfstrom and Hartmann, 2005; Head et al., 2010; Milliken et al., 2003; Hubbard et al., 2011) (Fig. 2c). These craters host gullies that are often partially or fully covered by LDM deposits and are also inferred to incise LDM deposits.

2. Bedrock: Craters where the features listed in criterion 1 (LDM/glacial deposits) are absent and where rocky material is visible extending downwards from the crater rim (Fig. 2d). This rocky material usually outcrops as spurs and can be layered or massive. The slopes can be smooth or covered with boulders, with concentrations of boulders at the slope toe.

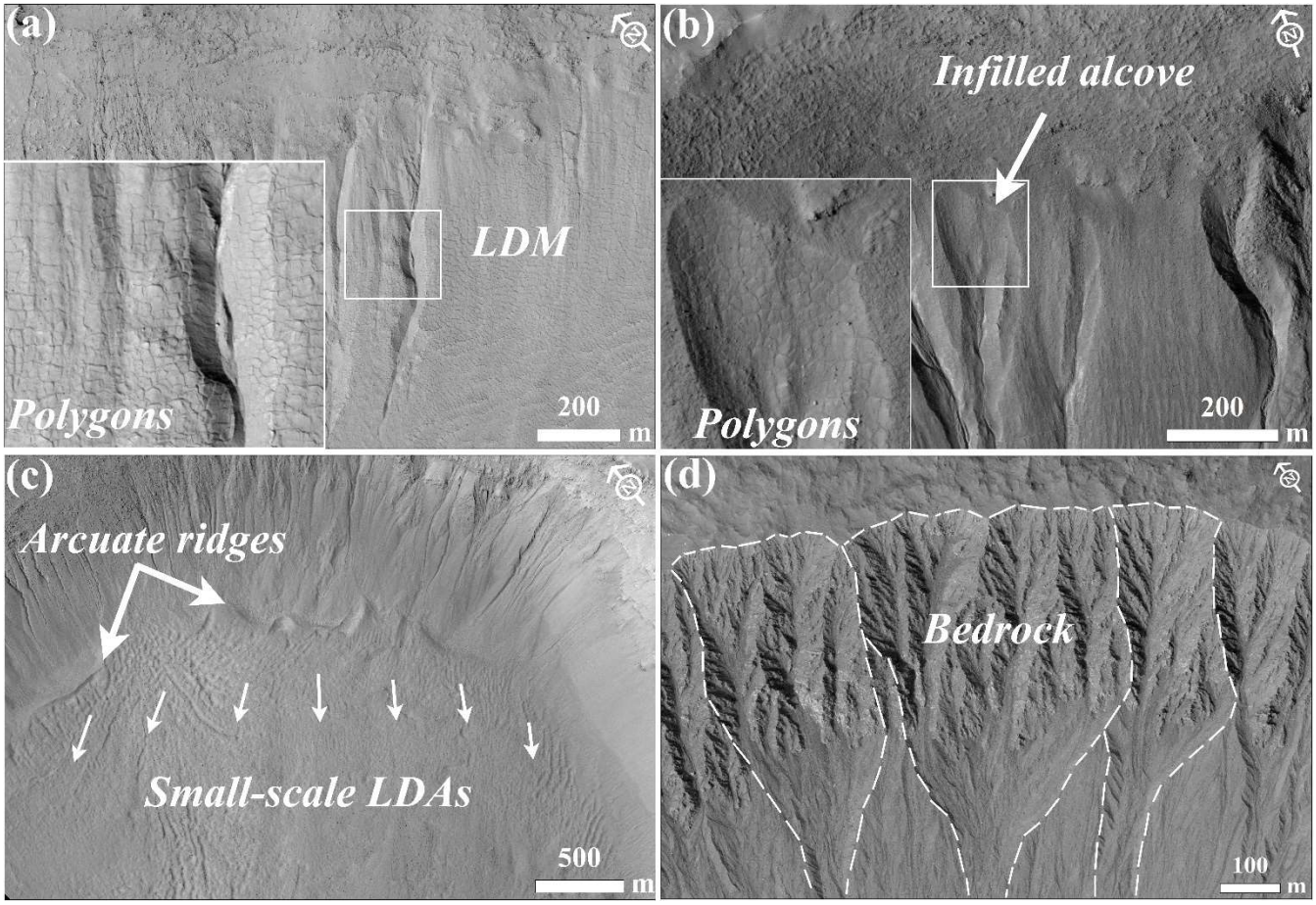

Figure 2: Examples of morphological evidence used to identify LDM, glacial deposits, and bedrock. (a) Smooth mantling material inferred as LDM draped on the wall of Talu crater on the basis of polygonal cracks formed in the material. The bigger box is an expanded view of the polygons seen over the region outlined by the smaller box. (HiRISE image ESP_011817_1395). (b) An infilled alcove on the wall of an unnamed crater-2 in Terra Sirenum. Polygons in the infilled material suggests presence of LDM deposits draped on the wall. The region shown in smaller box is expanded in the bigger box to show evidence of the polygons. (HiRISE image ESP_020407_1410). (c) Glaciation inferred in the Corozal crater on the basis of arcuate ridges formed at the foot of the crater wall and small-scale LDAs on the crater floor. Arrows indicate the downslope flow of LDAs on the floor. (HiRISE image PSP_006261_1410). (d) Exposed fractured bedrock identified on the walls of Istok crater within which gully alcoves have incised. The dashed lines show the gully systems that were investigated in this study. (HiRISE image ESP_056668_1345). HiRISE image credit: NASA/JPL /University of Arizona.

3.2 Morphometric variables

The measurements we made of each gully system include alcove area, alcove perimeter, alcove length, alcove width, alcove gradient, fan area, fan length, fan width, and fan gradient (Fig. 3). In total, we derived 18 morphometric variables to characterize each gully fan and its alcove. The morphometric variables are classified into geometry, relief, gradient, and dimensionless variables (e.g. form factor, elongation ratio, and circularity ratio) and they are calculated with established mathematical equations shown in Table 2. For the gradient measurement using the DTM, the topographic profile from (1) crest of the alcove to the apex of the fan was extracted for the alcove, and (2) apex to foot of the fan was extracted for the fan.

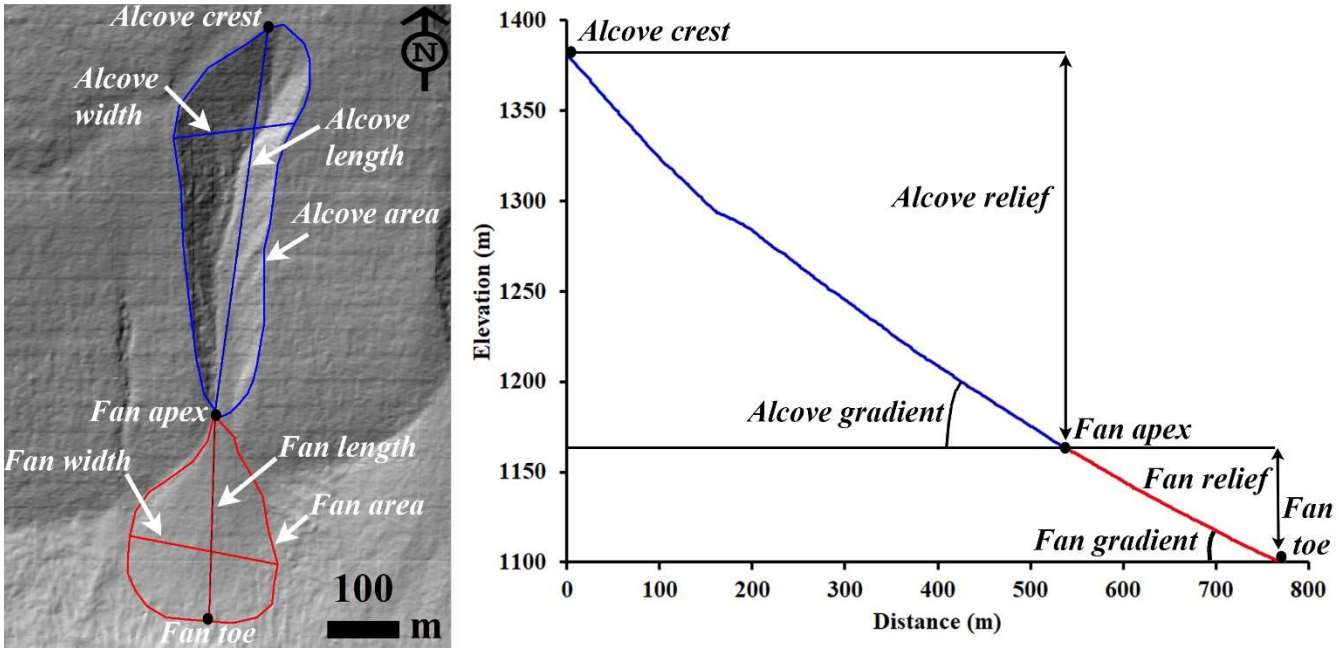

Figure 3: Examples of morphometric variables estimated in this work. Left panel: HiRISE DTM (Id: DTEEC_002659_1420_002514_1420) based hillshade. HiRISE DTM credit: NASA/JPL /University of Arizona. Right panel:

Topographic profile: blue profile represents the topography of gully alcove from alcove top to fan apex and red profile represents the profile of gully fan from fan apex to fan toe.

Table 2. Set of morphometric variables extracted from the studied gully systems and their formulas and/or description of method.

Morphometric variable	Formula and/or description of method	References
Alcove length and width	Measured in km	**Tomczyk, 2021**
Alcove area	Measured in km^2	**Tomczyk, 2021**
Fan length and width	Measured in km	**Tomczyk, 2021**
Fan area	Measured in km^2	**Tomczyk, 2021**
Melton ratio	(Alcove relief)/(Alcove area$^{-0.5}$)	**Melton, 1957**
Relative concavity index (RCI)	Concavity Index/(maximum relief between the uppermost and lowermost points along the gully fan profile/2). Concavity Index is estimated as $\sum (H_i^* - H_i) / N$, where H_i^* is the elevation along the straight line, H_i is the elevation along the gully fan profile, N is the total number of measurement points.	**Langbein, 1964; Phillips and Lutz, 2008**
Alcove gradient	Measured in (°)	**Tomczyk, 2021**
Fan gradient	Measured in (°)	**Tomczyk, 2021**
Alcove relief	Measured in km	**Tomczyk, 2021**
Fan relief	Measured in km	**Tomczyk, 2021**
Relief ratio (alcove and fan)	Alcove/fan relief divided by the length of the alcove/fan	**Schumm, 1956a, b**
Alcove Perimeter	Measured in km	**Schumm, 1956a, b**
Form factor	Alcove area divided by the square of the length of the alcove	**Horton, 1932**
Elongation ratio	Diameter of a circle of the same area as the alcove divided by the maximum alcove length	**Schumm, 1956a, b**
Circularity ratio	Alcove area divided by the area of the circle having the same perimeter as the alcove perimeter	**Miller, 1953**

3.3 Gully system selection for morphometric measurements

We have selected only those gully systems for morphometric measurements in which: (i) the depositional fan from an alcove-channel system is not superimposed by or interfingering with the fans from the neighboring channels, (ii) there is clear association between the primary channel emanating from the alcove that extends downslope and then deposit its respective fan, (iii) no evidence of extensive cross-cutting is seen with the neighboring channels on the walls, (iv) no evidence of extensive mantling by dust/aeolian deposits is apparent, and (v) no evidence of channel/fan superposition on any topographic obstacle on the walls or the floor of the crater is apparent, which may have influenced the morphometry. If in any case the fans

superimpose or channels cross-cut, we have carefully demarcated the alcove-channel-fan boundary, to minimize the inaccuracies in the measurements. Note that the selection of the gully systems was also constrained by the coverage of HiRISE DTMs used for morphometric analysis.

3.4 Statistical analysis of morphometric variables

We have two groups of gullies in our study: (1) gullies whose source areas are incised into LDM/glacial deposits and (2) gullies whose source areas are incised into the bedrock. First, for both the groups we have calculated descriptive statistics for each of the morphometric variables shown in Table 2. The significance of the difference between the values of each of the morphometric variables calculated for each group was tested using a Student's t-test. To apply t-tests, we have transformed the morphometric variables to remove skewness by taking their natural logarithm. Pearson correlation analysis has been used to investigate the correlation between the selected morphometric attributes of gully alcoves and fans. We infer strong positive correlations between variables if the correlation coefficient value is more than 0.7 and strong negative correlations if the value is less than -0.7. Very strong positive correlation between variables is inferred if the correlation coefficient is $\geq$0.9. Further, we used canonical discriminant analysis (CDA) to determine morphometric variables that provide the most discrimination between the groups of gullies. In CDA, functions are generated according to the number of groups, until a number equal to n-1 functions is reached (n is the number of groups) (McLachlan, 2005). For the two groups of gullies in our study, there is going to be a function for which there is a standardised canonical discriminant function coefficient associated with the morphometric variable. The higher the magnitude of this coefficient for a particular morphometric variable, the higher the role of that variable in separating the groups of gullies (Conway et al., 2015). Standardisation was done by dividing each value for a given variable by the maximum value.

4 Results

4.1 Morphology of gully systems

Out of the 29 gullied craters analysed in this work, we have found that there are 24 craters influenced by LDM and/or VFFs. The remaining 5 craters have gullies incised into the exposed underlying bedrock on the wall of the crater. Below we describe the substrates identified in the studied craters and then compare the morphology of the gullies formed into those substrates.

4 craters out of 24 craters (i.e. Raga, Roseau, unnamed crater in Newton basin and unnamed crater-1 in Terra Sirenum) have gullies that are only influenced by LDM. In these craters, we have found morphological evidence of LDM in the form of polygonized, smooth textured material on the pole-facing walls of the craters. Morphological evidence of VFF is not evident in these craters. In these craters, the gully-alcoves and gully channels appear to have been incised into the polygonized LDM material, and the gully-fan deposits are mantled. A typical example of this can be found in the unnamed crater formed inside the Newton basin (Fig. 4a). Roseau crater, in particular, contains a large number of gully systems whose alcoves and fans are

extensively mantled (Fig. 4b). The remaining 20 out of 24 craters contain evidence for gullies that are influenced by both LDM and glacial deposits (Table 1). The base of the pole-facing walls and the floor of the craters within which the gully systems have formed host linear-to-sinuous arcuate ridges and VFFs, respectively. Typical examples of VFFs can be found in Corozal, Talu, unnamed craters in Terra Sirenum and Argyre basin, Langtang, Dechu and Dunkassa craters (Fig. 4c). In majority of the gullied craters (except Raga, Roseau and unnamed crater-1 in Terra Sirenum) influenced by LDM and glacial deposits, gully alcoves are found to have a distinctive V-shaped cross section in their mid-section (Figures 4d and 4e), they do not extend up

to the crater rim, and gully systems often show multiple episodes of activity, inferred by the presence of fresh channel incision on the gully-fan surfaces (Fig. 4d-e).

Istok, Galap, Gasa, Los, and an unnamed crater in the Terra Sirenum contain gully systems on the pole-facing walls that are not associated with LDM and VFFs (Table 1). The gully alcoves inside these craters have a crenulated shape and appear to have formed by headward erosion into the bedrock of the crater rim (Fig. 4f). These craters have formed large gully systems on their pole-facing walls, with brecciated alcoves, comprising of multiple sub-alcoves and hosting many clasts/boulders (Fig. 4f).

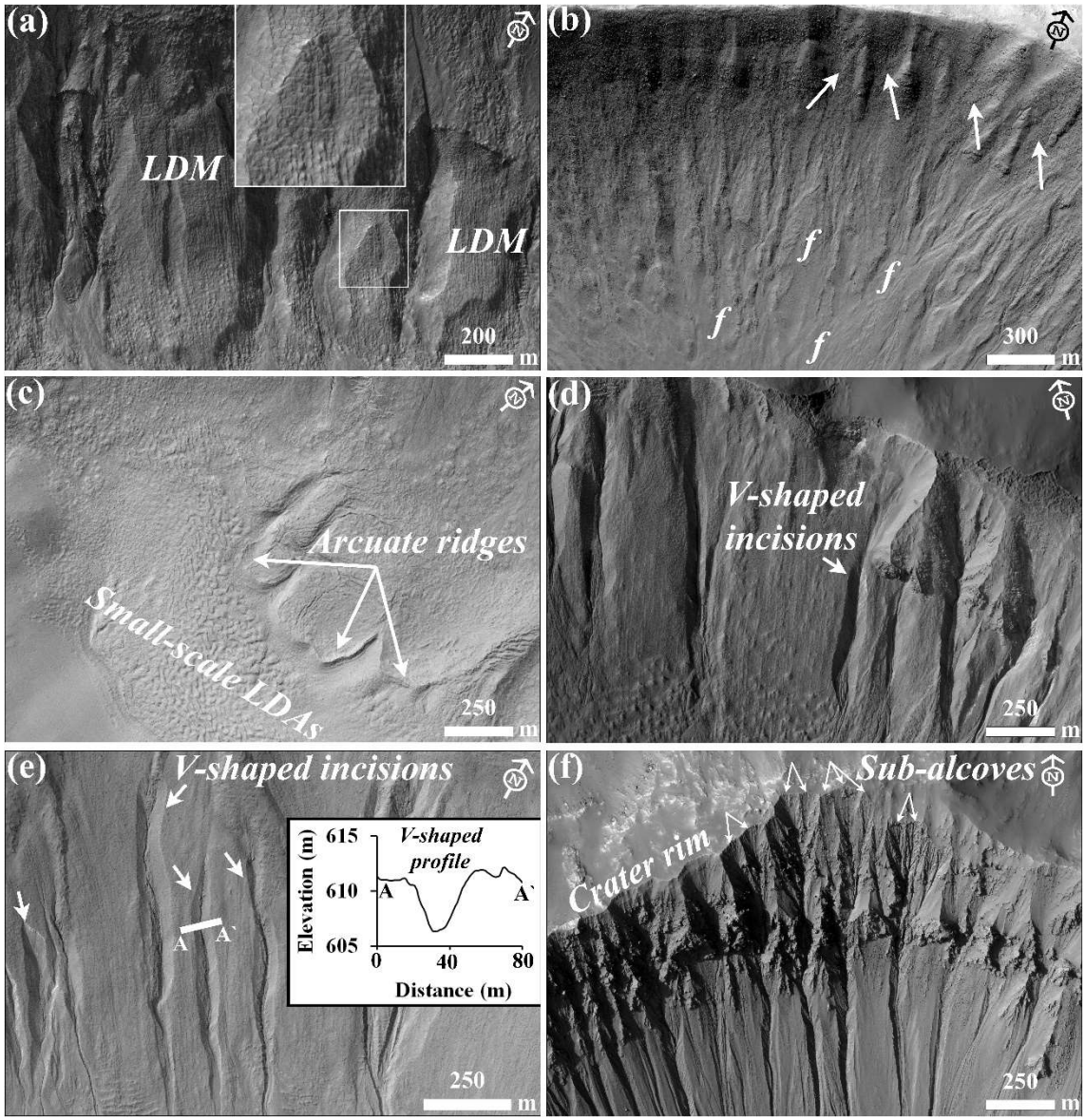

Figure 4: (a) LDM draped on the wall of an unnamed crater in the Newton basin. The inset shows details of the polygonal texture of the LDM. (HiRISE image PSP_002686_1410). (b) Infilled gully alcoves (arrows) and mantled fan surfaces (marked by letter 'f') on the wall of Roseau crater. (HiRISE image ESP_024115_1380). (c) Arcuate ridges at the foot of the crater wall and small-scale LDAs on the floor in Langtang crater. (HiRISE image ESP_030099_1415). (d) V-shaped incisions on the LDM draped walls of Taltal (HiRISE image ESP_037074_1400) and (e) Langtang crater (HiRISE image ESP_030099_1415). Note the topographic profile (A-A`) that illustrates V-shaped incision of the gully channel. (f) Gully alcoves formed in Los crater by headward erosion into the crater rim. Individual gully alcoves formed in bedrock have multiple sub-alcoves. (HiRISE image ESP_020774_1445).

4.2 Morphometry of gully systems

Based on the criteria summarized in section 3.3, we have studied 167 gullies across 29 craters for calculation of morphometric variables. 130 gullies are formed within LDM/glacial deposits, and 37 gullies are formed within the bedrock. The results of morphometric calculations are summarized for visual comparison as a boxplot (Fig. 5).

The results of the Student's t-test indicates that all of the morphometric variables in Table 2, except fan width, fan area, Melton ratio, form factor, elongation ratio, and circularity ratio, differ significantly between LDM/glacial deposits and bedrock (Fig. 5). Compared to the mean gradient of gully-fans formed in LDM/glacial deposits, bedrock gully-fans are steeper and possess a higher relief ratio. The interquartile range of length, relief, and perimeter of gully alcoves formed in bedrock are also higher than the interquartile range of similar variables in LDM/glacial deposits, but the gully alcoves in LDM/glacial deposits possess much higher values of length, relief, and perimeter (Fig. 5).

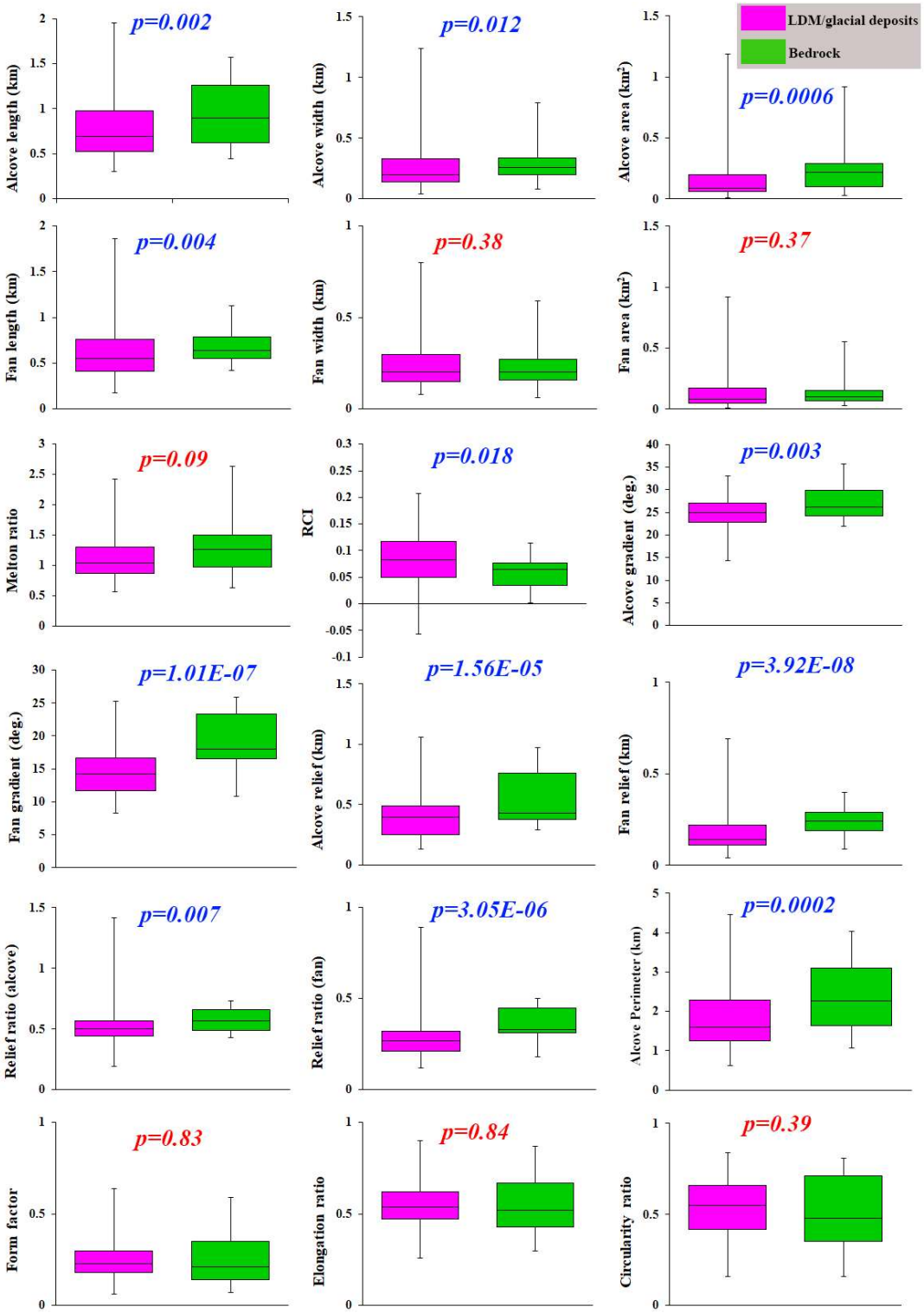
LDM/glacial deposits
Bedrock
Alcove length (km)
p=0.002
Alcove width (km)
p=0.012
Alcove area (km²)
p=0.0006
Fan length (km)
p=0.004
Fan width (km)
p=0.38
Fan area (km²)
p=0.37
Melton ratio
p=0.09
RCI
p=0.018
Alcove gradient (deg.)
p=0.003
Fan gradient (deg.)
p=1.01E-07
Alcove relief (km)
p=1.56E-05
Fan relief (km)
p=3.92E-08
Relief ratio (alcove)
p=0.007
Relief ratio (fan)
p=3.05E-06
Alcove Perimeter (km)
p=0.0002
Form factor
p=0.83
Elongation ratio
p=0.84
Circularity ratio
p=0.39

Figure 5: The boxplot presented here shows interquartile range, central horizontal bar shows median, and whiskers show range of values of alcove/fan geometry, relief, gradient, and dimensionless variables of gullies incised into LDM/glacial deposits (pink) and bedrock (green). P-values on the plots represent the results of the student's t-tests for testing the significance of difference in means of the morphometric variables between gully systems formed on LDM/Glacial deposits and bedrock. P-values in blue correspond to significant difference (with respect to a p-value of 0.05) and those in red are non-significant.

Pearson correlations between morphometric attributes of gully alcoves and fans formed in bedrock and LDM/glacial deposits are summarized in Fig. 6. For bedrock, there are strong positive correlations between 12 pairs of morphometric variables and strong negative correlations between 3 pairs of morphometric variables. For LDM/glacial deposits, there are strong positive correlations between 18 pairs of morphometric variables and strong negative correlations between 3 pairs of morphometric variables. Very strong positive correlations (>0.9) are found between 9 pairs of morphometric variables for bedrock and between 4 pairs of morphometric variables for LDM/glacial deposits.

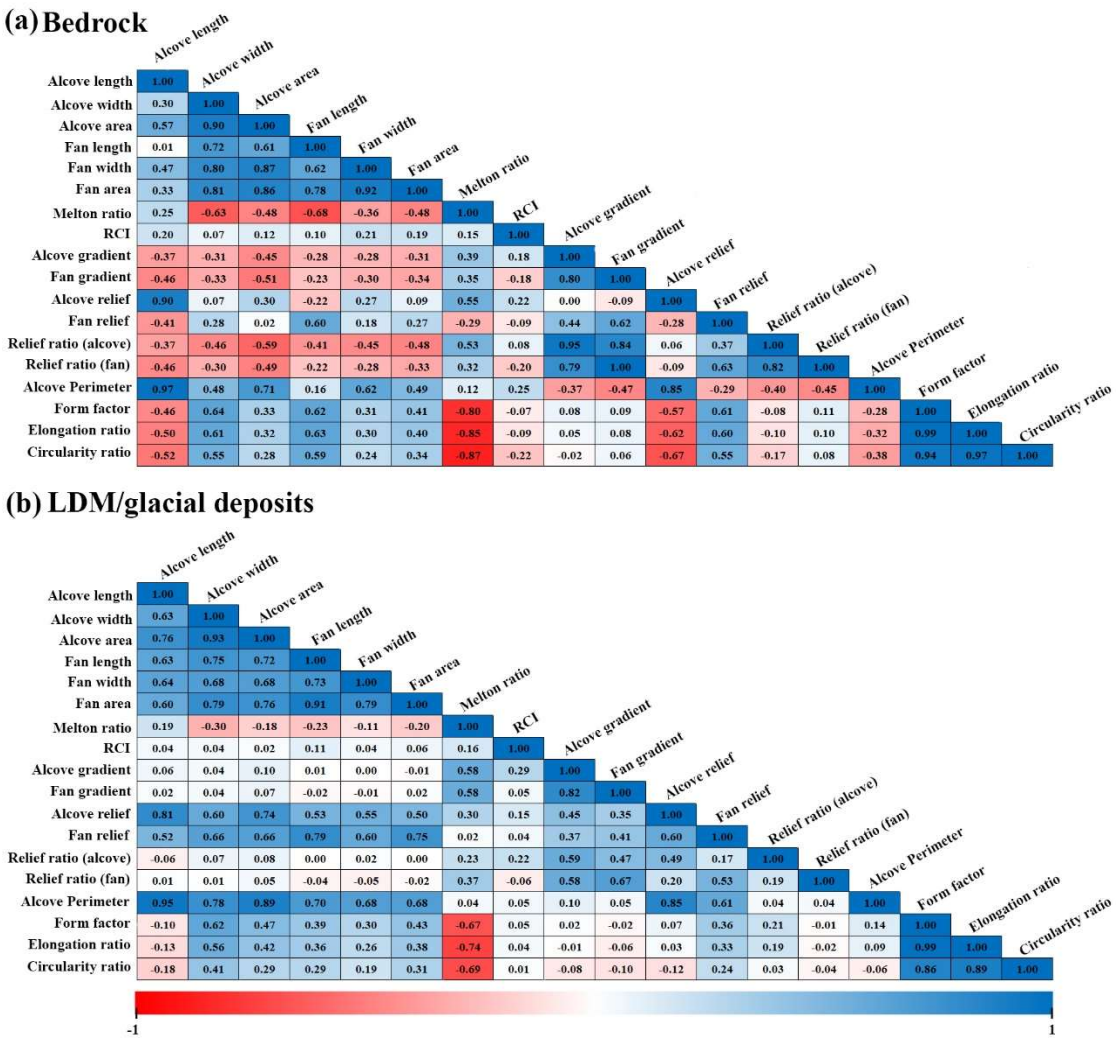

Figure 6: Pearson correlations between morphometric attributes of gully alcoves and fans formed in (a) bedrock and (b) LDM/glacial deposits. Values approaching either 1 or -1 have stronger correlations. Zero indicates no correlation.

The canonical discriminant analysis reveals that the following morphometric variables best distinguish between the gully systems formed in LDM/glacial deposits and bedrock, in descending order of importance: alcove perimeter, alcove relief, fan gradient, fan relief, fan length, relief ratio (alcove), alcove width, relief ratio (fan), alcove gradient, alcove area, alcove length, and relative concavity index (Table 3). The alcove perimeter is most important in discriminating among the gully systems formed within LDM/glacial deposits and bedrock, and the next two most important variables are alcove relief and fan gradient. Alcove relief and fan gradient have 4/5 and 1/3 the weight of alcove perimeter, respectively. Here, the weight values indicate

the discriminator power in separating between the gullies formed in LDM/glacial deposits and bedrock. The remaining variables such as fan relief, fan length, relief ratio (alcove), alcove width, and relief ratio (fan) have nearly 1/5 or greater (but less than 1/3) of the weight of alcove perimeter discriminatory power in separating between the gullies formed in LDM/glacial deposits and bedrock. The variables with the smallest magnitude, alcove gradient, alcove area, alcove length and relative concavity index, have less than 1/10 the weight of the most important variable in separating the gully systems.

Table 3. Standardised canonical discriminant function coefficients (F1) that best separate gully systems formed on LDM/Glacial deposits and bedrock.

Variable	F1
Alcove Perimeter	3.552
Alcove relief	-2.828
Fan gradient	1.278
Fan length	-1.06
Fan relief	1.06
Relief ratio (alcove)	0.971
Alcove width	-0.692
Relief ratio (fan)	-0.665
Alcove gradient	-0.331
Alcove area	-0.319
Alcove length	0.23
Relative concavity index	-0.182

5 Discussion

5.1 Unique morphology and morphometry of gully systems in different substrates

We have found that the gully systems formed in LDM/glacial deposits and bedrock can, using discriminatory analysis, be distinguished from one another in terms of perimeter and relief of gully alcoves (Table 3). Additionally, we have found statistically significant difference between the perimeters and reliefs of gully alcoves formed in LDM/glacial deposits and bedrock (Fig. 5). It is likely that these differences in the perimeters and reliefs of gully alcoves formed within morphologically distinct substrates could be due to the integral nature of the surface material within which the gully alcoves have formed. In other words, it is possible that the differences in the physical properties of the sediments (namely grain size, compactness etc.) within which gully alcoves have formed played a key role in erosion of the substrate leading to differences in their

morphometric variables. Below we elaborate on the uniqueness of the substrates within which gully alcoves have formed, and discuss further the relationships between the morphometric variables of the morphologically distinct gully systems.

On Mars, VFFs contain high purity glacial ice with a debris cover (Sharp, 1973; Squyres, 1978, 1979; Squyres and Carr, 1986; Holt et al 2008, Plaut et al 2009, Petersen et al. 2018). Their surfaces have been interpreted to comprise of finer, reworked debris derived from sublimation of the underlying ice (Baker et al., 2010; Plaut et al., 2009). The smooth, meters thick draping unit on the walls of formerly glaciated craters has been suggested to be derived from the atmosphere as a layer of dust-rich ice primarily constituting of fine-grained materials (Kreslavsky and Head, 2000; Mustard et al., 2001). The fine-grained materials are loosely-packed, unconsolidated materials exhibiting low thermal inertia values (Mellon et al., 2000; Putzig et al., 2005). Typically, gullies formed within this substrate display a smooth surface texture, wherein, evidence of individual clasts or meter-scale boulders is not resolvable in HiRISE images, substantiating the dominant component of fine-grained materials within the LDM (e.g., Levy et al., 2010; de Haas et al., 2015a). Additionally, it has been found that gully alcoves incised into the LDM always have a distinctive V-shaped cross section in their mid-section (Figures 4d and 4e), which when compared with similar-scaled systems on Earth also corresponds to the presence of loose sediments constituting the LDM (Conway et al., 2018). The gully alcoves with V-shaped cross sections are found to be elongated, likely indicating incision within ice-rich unlithified sediments (Aston et al., 2011). In the studied craters, we have found that gullies incised into LDM/glacial deposits do have an elongated, V-shaped cross section in their mid-sections (Fig. 4). We propose that the presence of fine-grained, loosely packed, unconsolidated materials within LDM/glacial deposits has facilitated formation of elongated gully alcoves with perimeters and reliefs relatively higher than that of gully alcoves formed in coarse-grained bedrock substrate. This is consistent with the previous studies suggesting that gullies eroding into LDM/glacial deposits have elongated catchments (Aston et al., 2011), whereas gullies eroding into the bedrock have more amphitheater-shaped catchments (Levy et al., 2009b). For this reason, the estimated length of gully alcoves formed in LDM/glacial deposits is found to be relative higher than that of gully alcoves formed in bedrock (Fig. 5). Furthermore, statistical analysis has revealed a significant difference between the length of gully alcoves formed in LDM/glacial deposits and bedrock (Fig. 5). Additionally, the presence of finer-grained sediments in LDM/glacial deposits is the likely cause of the V-shape of the incision of gully alcoves investigated in this study (Aston et al., 2011). On Earth, V-shaped incisions through glacial ice-rich moraines have been observed to have occurred during the paraglacial phase of glacial retreat (Bennett et al., 2000; Ewertowski and Tomczyk, 2015) (Fig. 7). The paraglacial phase refers to a terrestrial post-glacial period that represents the response of changing environment to deglaciation (Bennett et al., 2000; Ewertowski and Tomczyk, 2015).

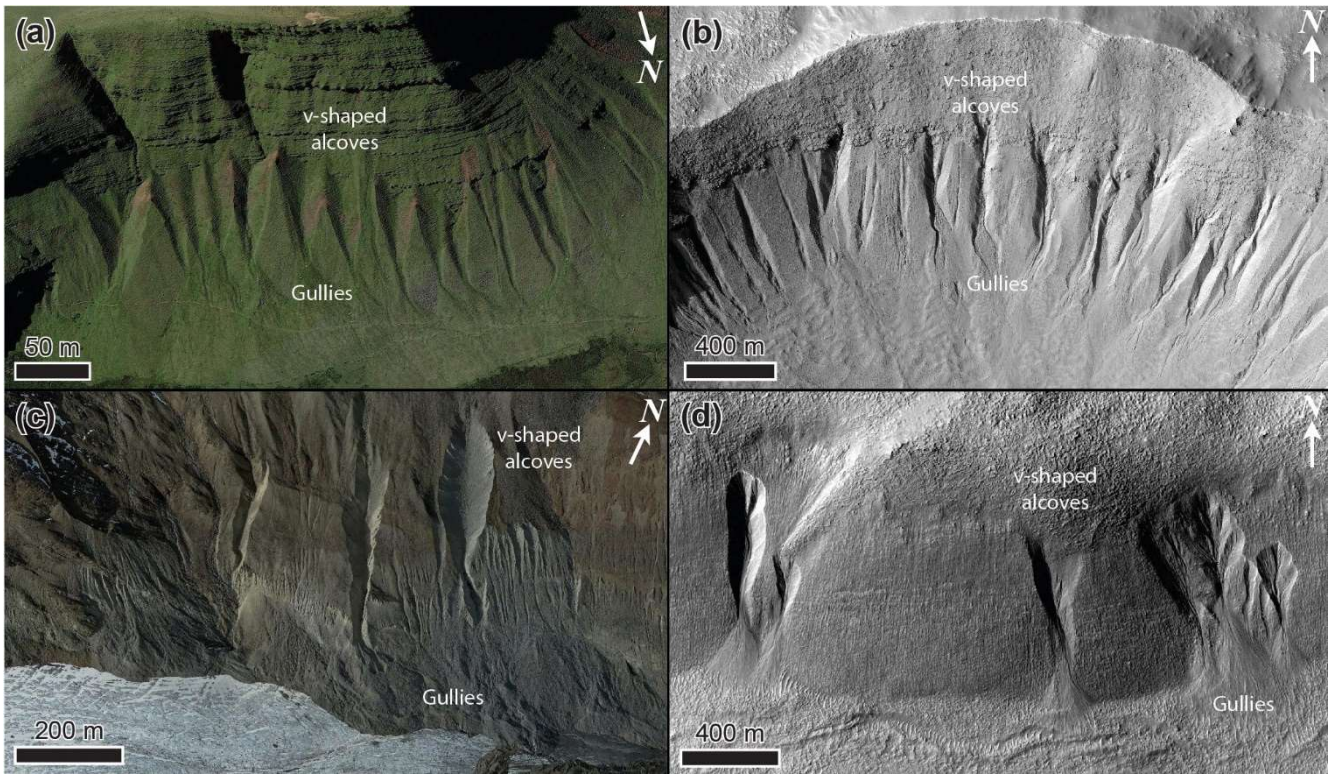

Figure 7: Gullies forming in glacial sediments in deglaciated terrain in the (a) Brecon Beacons, Wales, UK on Earth (Google Earth coordinates: 51°52'59.11"N, 3°43'33.26"W), (b) Talu crater (https://www.uahirise.org/ESP_011817_1395) on Mars, (c) Hintereisferner, Austria (Google Earth coordinates: 46°48'54.25"N, 10°47'8.18"E), on Earth, and (d) Bunnik crater (https://www.uahirise.org/ESP_047044_1420) on Mars. HiRISE image credit: NASA/JPL-Caltech/University of Arizona.

The next most important difference between these two types of gullies is the mean gradient of gully fans. At the foot of the fans, mean gradient of the fans influenced by LDM/glacial deposits is <15° for 61% of the studied fans. For bedrock, 84% of the studied fans have a mean gradient >15° at the foot of the fans. Hence, gully-fans formed in bedrock are emplaced at a relatively steeper gradient than the fans formed from gullies in LDM/glacial deposits. We propose that the nature of the material mobilized can explain this difference, with the finer-grained sediments characteristic of the LDM/glacial type gullies being easier to mobilise and being entrained to lower slope angles, than the coarser sediments found within the bedrock type gullies.

5.2 Evaluation of the gully formation process

On Earth, alcove-fan systems can roughly be subdivided in flood-dominated, debris-flow dominated, and colluvial systems. Following the terminology of De Haas et al., (2015b) and Tomczyk (2021), we define these systems as follows:

1) Flood-dominated systems: These are systems dominated by fluid-gravity flows, i.e., water floods, hyperconcentrated floods, and debris floods. The fans of such systems are commonly referred to as fluvial or alluvial fans (e.g., Ryder, 1971; Blair and McPherson, 1994; Hartley et al., 2005).

2) Debris-flow dominated systems: These are systems dominated by sediment-gravity flows, i.e., debris flows, mud flows. Irrespective of their radial extent and depositional gradients, the fans aggraded by these systems can be commonly called debris-flow fans or debris fans (Blikra and Nemec, 1998; de Scally et al., 2010).

3) Colluvial systems: These are systems dominated by rock-gravity and sediment-gravity flows, with their dominant activity relating to rockfalls, grain flows, and snow avalanches (in periglacial and alpine settings). Debris flows typically constitute only a relatively minor component of geomorphic processes in such systems. The fans of these systems are also commonly known as colluvial cones or talus cones (Siewert et al., 2012; De Haas et al., 2015b).

Although these systems may be dominated by one type of geomorphic process, it is important to stress that other processes may also occur. For example, on Earth water floods are not uncommon on many debris-flow dominated systems, while debris-flow deposits are commonly recognized on colluvial cones.

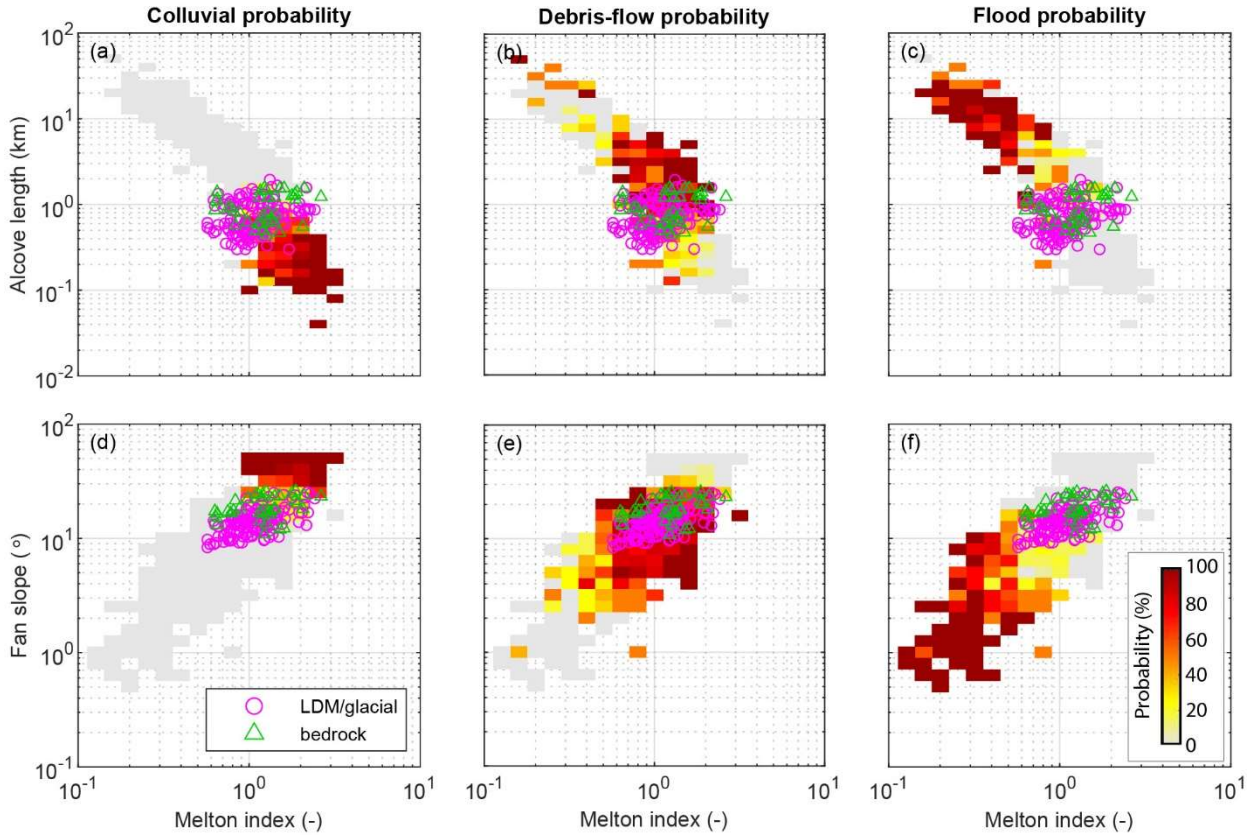

Figure 8: Comparison of combinations of Melton ratio with Alcove length and Fan gradient. The probability heat maps are based on previously published data – see text for references. The Martian gully systems formed in LDM/glacial deposits and bedrock are found to be in the debris-flow regime on Earth. The gray area shows the realm of the colluvial, debris-flow, and fluvial fans together.

To compare the morphometric characteristics of the Martian gully systems to terrestrial systems, we have compiled morphometric data of gully alcoves and fans across several continents, mountain ranges, climate zones, and process types on Earth. This dataset includes published data from the Himalayas, Ladakh, India (Stolle et al., 2013), the tropical Andes, Columbia (Arango et al., 2021), Spitsbergen, Svalbard (Tomczyk, 2021), British Columbia, Canada (Kostaschuk, 1986; Jackson et al., 1987; and newly presented data), the southern Carpathians, Romania (Ilinca et al., 2021), the Southern Alps, New Zealand (De Scally and Owens, 2004; De Scally et al., 2010), the North Cascade Foothills, USA, the European Alps (including Switzerland, Italy, France, and Austria), and the Pyrenees (from multiple authors compiled by Bertrand et al., 2013). The dataset comprises information from colluvial, debris-flow, and flood (also including debris flood) dominated systems. In

total, it contains 231 colluvial systems, 749 debris-flow dominated systems, and 369 flood-dominated systems. In total, data were compiled for 1349 systems, although not all information was available for all systems, with data availability ranging from 729 sites for alcove length to all 1349 systems for Melton index and process type. Based on this data we have made a heatmap of the probability of flood, debris-flow, or colluvially-dominated conditions for combinations of Melton ratio with alcove length and fan gradient, to which we compare the Martian gullies (Fig. 8). We have specifically chosen the combinations of Melton ratio with alcove length and fan gradient to infer the Martian gully formative mechanism because they have been widely used in discriminating terrestrial drainage basins and fans prone to flooding from those subject to debris flows, debris floods and floods (e.g. De Scally and Owens, 2004; Wilford et al., 2004). We have found that the Martian gullies are indeed in the debris-flow regime on Earth. Moreover, they are closer to the transition to the smaller and steeper colluvial cones than to transition to flood-dominated fans. As expected, bedrock systems in Fig. 8d-e are closer to the colluvial systems than the LDM systems.

According to the previous reports of debris-flow like deposits found in Martian gullies (e.g. Johnsson et al., 2014; Sinha et al., 2019, 2020), the morphological attributes of debris-flow like deposits typically include overlapping tongue-shaped lobes with embedded clasts, channels with medial deposits, and channels with clearly defined lateral levees. Although it is still not clear whether the formation of these deposits in gullies are from sublimation of CO_2 ice or due to meltwater generation. De Haas et al., (2019b) showed that CO_2 sublimation may lead to flow fluidization on Mars in a manner similar to fluidization by water in terrestrial debris flows; a concept supported by the recent finding of lobate deposits and boulder-rich levee formation during the present-day in Istok crater (Table 1) (Dundas et al., 2019). The formation of these morphologically similar deposits during the present-day is attributed to sublimating CO_2 frost, which likely produces the necessary fluidization likely by gas generated from entrained CO_2 frost (Dundas et al., 2019). On the basis of these recent reports (De Haas et al., 2019b; Dundas et al., 2019) and based on our own findings in this study, we argue that a debris-flow like process similar to those operated in the terrestrial gully systems has likely dominated the flow types that lead to gully formation on Mars. Present-day sublimation of CO_2 ice on Mars may have provided the necessary flow fluidization for the emplacement of deposits similar to terrestrial debris-flow like deposits (De Haas et al., 2019b).

6 Conclusions

This paper compares morphological and morphometric characteristics of gully alcoves and associated fans formed in LDM/glacial deposits and bedrock over walls of 29 craters between 30° S and 75° S latitudes on Mars. 5 craters out of 29 have alcoves-fans formed within the bedrock and remaining 24 craters have alcoves-fans formed within LDM/glacial deposits. From our analysis of 167 gullies, we posit that gully systems formed in LDM/glacial deposits and bedrock differ from one another using the following lines of evidence:

• Gully alcoves formed in LDM/glacial deposits are more elongated than the gully alcoves formed in bedrock, and possess a distinctive V-shaped cross section.

• The mean gradient of gully-fans formed in bedrock is steeper than the mean gradient of fans formed from gullies in LDM/glacial deposits.

The morphological distinction reported between gullies formed in the bedrock and LDM/glacial deposits signifies that Martian gullies may have multiple formative environments. We infer that the presence of mantling material could be one of the key factors in constraining the mechanisms forming Martian gully systems and that presence of LDM would promote formation of elongated gully alcoves with perimeters and reliefs relatively higher than that of gully alcoves formed in coarse-grained bedrock substrate.

Based on the combinations of Melton ratio with alcove length and fan gradient, we suggest that the gully systems studied in this work were likely dominated by terrestrial debris-flow like processes during their formation. This is consistent with the findings reported in previous studies that showed evidence of formation of deposits morphologically similar to terrestrial debris-flow like deposits, both in the past and during the present-day (e.g., Johnsson et al., 2014; Dundas et al., 2019). The present-day sublimation of CO_2 ice on Mars is envisaged to provide the necessary flow fluidization for the emplacement of deposits similar to debris-flow like deposits on Earth (De Haas et al., 2019b).

7 Author contribution

RKS, TDH and SJC conceptualized this work. The methodology was developed by RKS, TDH and SJC. Data curation and formal analyses were performed by RKS. TDH and AN also contributed in collection of datasets used in this work. RKS, DR, TDH and SJC contributed to the interpretation of the data and results. RKS wrote the original draft of this paper, which was reviewed and edited by all authors.

8 Conflict of interest

SJC is a Guest Editor of this special issue (Planetary landscapes, landforms, and their analogues) of ESurf and on the editorial board for ESurf. The peer-review process was guided by an independent editor, and the authors have also no other competing interests to declare.

9 Acknowledgements

We are grateful and thank both the anonymous reviewers for thorough assessment of our manuscript and for providing us constructive comments and suggestions. Thanks to the Editor (Heather Viles) and Associate Editor (Frances E. G. Butcher) at Earth Surface Dynamics for the editorial handling of the manuscript. We would like to thank the HiRISE team for their work to produce the images and digital elevation models used in this study, it would have been impossible without them. RKS and

DR acknowledge the financial support by the Indian Space Research Organisation, Department of Space, Government of India. SJC and AN are grateful for the financial support from Région Pays de la Loire, project étoiles montantes METAFLOWS (convention N° 2019-14294) and also the financial support of CNES in support of their HiRISE work. TdH was supported by the Netherlands Organisation for Scientific Research (NWO) (grant 016.Veni.192.001). We acknowledge the efforts of team MUTED to develop an online tool (http://muted.wwu.de/) for quick identification of the spatial and multi-temporal coverage of planetary image data from Mars. All the planetary datasets used in this work are available for free download at the PDS Geosciences Node Mars Orbital Data Explorer (ODE) (https://ode.rsl.wustl.edu/mars/) and https://www.uahirise.org/. The newly-generated DTMs can be downloaded from **https://figshare.com/articles/dataset/Self_generated_DEMs/21717164.** The measurement datasets can be downloaded from **https://figshare.com/articles/dataset/Measurement_data_of_gully_systems_in_the_southern_mid_latitudes_of_Mars/21717182**. This work is a part of the PhD work of Rishitosh K. Sinha. Director PRL, Head of Planetary Science Division, PRL, Head of Planetary Remote Sensing Section, PRL, and Director IIT Gandhinagar are gratefully acknowledged for constant encouragement during the work.

References

Arango, M. I., Aristizábal, E., & Gómez, F.: Morphometrical analysis of torrential flows-prone catchments in tropical and mountainous terrain of the Colombian Andes by machine learning techniques, Natural Hazards, 105(1), 983-1012, doi: https://doi.org/10.1007/s11069-020-04346-5, 2021.

Arfstrom, J. & Hartmann, W.K.: Martian flow features, moraine-like ridges, and gullies: terrestrial analogs and interrelationships, Icarus, 174, 321–335, doi: https://doi.org/10.1016/j.icarus.2004.05.026, 2005.

Aston, A., Conway, S. & Balme, M.: Identifying Martian Gully Evolution. In: Balme, M.R., Bargery, A.S., Gallagher, C.J. & Gupta, S. (eds) Martian Geomorphology, Geological Society, London, Special Publications, 356, 151–169, doi: https://doi.org/10.1144/SP356.9, 2011.

Baker, D. M. H, James W. H., and David R. M.: Flow patterns of lobate debris aprons and lineated valley fill north of Ismeniae Fossae, Mars: Evidence for extensive mid-latitude glaciation in the Late Amazonian, Icarus 207, 186-209, 2010, doi: https://doi.org/10.1016/j.icarus.2009.11.017.

Balme, M., Mangold, N. Et Al.: Orientation and distribution of recent gullies in the southern hemisphere of Mars: observations from High Resolution Stereo Camera/Mars Express (HRSC/MEX) and Mars Orbiter Camera/Mars Global Surveyor (MOC/MGS) data, J. Geophys. Res.: Planets, 111, E05001, doi: https://doi.org/10.1029/2005JE002607, 2006.

Bertrand, M., Liébault, F., & Piégay, H.: Debris-flow susceptibility of upland catchments, Natural Hazards, 67(2), 497-511, doi: https://doi.org/10.1007/s11069-013-0575-4, 2013.

520 Blair, T.C. & Mcpherson, J.G.: Processes and forms of alluvial fans. In: PARSONS, A. & ABRAHAMS, A. (eds)
521 Geomorphology of Desert Environments, Springer, Dordrecht, The Netherlands, 413–467, doi: https://doi.org/10.1007/978-1-
522 4020-5719-9_14, 2009.

523 Blair, T.C.: Sedimentology of the debris-flow-dominated Warm Spring Canyon alluvial fan, Death Valley, California,
524 Sedimentology 46 (5), 941–965, doi: https://doi.org/10.1046/j.1365-3091.1999.00260.x, 1999.

525 Blikra, L.H., Nemec, W.: Postglacial colluvium in western Norway: depositional processes, facies and palaeoclimatic record.
526 Sedimentology 45 (5), 909–960, doi: https://doi.org/10.1046/j.1365-3091.1998.00200.x, 1998.

527 Cedillo-Flores, Y., Treiman, A.H., Lasue, J. & Clifford, S.M.: CO2 gas fluidization in the initiation and formation of Martian
528 polar gullies, Geophys. Res. Letters, 38, L21202 doi: https://doi.org/10.1029/2011GL049403, 2011.

529 Christensen, P.R.: Formation of recent Martian gullies through melting of extensive water-rich snow deposits, Nature, 422,
530 45–48, doi: https://doi.org/10.1038/nature01436, 2003.

531 Conway, S. J., Butcher, F. E., de Haas, T., Deijns, A. A., Grindrod, P. M., & Davis, J. M.: Glacial and gully erosion on Mars:
532 A terrestrial perspective, Geomorphology, 318, 26-57, doi: https://doi.org/10.1016/j.geomorph.2018.05.019, 2018.

533 Conway, S.J. & Balme, M.R.: Decameter thick remnant glacial ice deposits on Mars, Geophys. Res. Letters, 41, 5402–5409,
534 doi: https://doi.org/10.1002/2014GL060314, 2014.

535 Conway, S.J., Balme, M.R., Kreslavsky, M.A., Murray, J.B. & Towner, M.C.: The comparison of topographic long profiles
536 of gullies on Earth to gullies on Mars: a signal of water on Mars. Icarus, 253, 189–204, doi:
537 https://doi.org/10.1016/j.icarus.2015.03.009, 2015.

538 Conway, S.J., Balme, M.R., Murray, J.B., Towner, M.C., Okubo, C.H. & Grindrod, P.M.: The indication of Martian gully
539 formation processes by slope–area analysis, In: Balme, M.R., Bargery, A.S., Gallagher, C.J. & Gupta, S. (eds) Martian
540 Geomorphology, Geological Society, London, Special Publications, 356, 171–201, doi: https://doi.org/10.1144/SP356.10,
541 2011.

542 Conway, S.J., Harrison, T.N., Soare, R.J., Britton, A.W. & Steele, L.J.: New slope-normalized global gully density and
543 orientation maps for Mars, In: Conway, S.J., Carrivick, J.L., Carling, P.A., De Haas, T. & Harrison, T.N. (eds) Martian Gullies
544 and their Earth Analogues, Geol. Soc. Lond. Spec. Publ. 467. First published online November 27, 2017, doi:
545 https://doi.org/10.1144/SP467.3, 2017.

546 Costard, F., Forget, F., Mangold, N. & Peulvast, J.P.: Formation of recent Martian debris flows by melting of near-surface
547 ground ice at high obliquity, Science, 295, 110–113, doi: 10.1126/science.1066, 2002.

548 Crosta, G.B., Frattini, P.: Controls on modern alluvial fan processes in the central Alps, northern Italy, Earth Surf. Proc. Land.
549 29 (3), 267–293, doi: https://doi.org/10.1002/esp.1009, 2004.

550 de Haas, T., Conway, S.J., Butcher, F.E.G., Levy, J.S., Grindrod, P.M., Balme, M.R., Goudge, T.A.: Time will tell: temporal
551 evolution of Martian gullies and paleoclimatic implications, Geol. Soc. Lond. Spec. Publ. 467, doi:
552 https://doi.org/10.1144/SP467.1, 2019a.

553 de Haas, T., McArdell, B. W., Conway, S. J., McElwaine, J. N., Kleinhans, M. G., Salese, F., & Grindrod, P. M.: Initiation
554 and flow conditions of contemporary flows in Martian gullies, J. Geophys. Res.: Planets, 124(8), 2246-2271, doi:
555 https://doi.org/10.1029/2018JE005899, 2019b.

556 de Haas, T., Hauber, E. & Kleinhans, M.G. 2013. Local late Amazonian boulder breakdown and denudation rate on Mars,
557 Geophys. Res. Letters, 40, 3527–3531, doi: https://doi.org/10.1002/grl.50726, 2013.

558 de Haas, T., Ventra, D., Hauber, E., Conway, S.J. & Kleinhans, M.G.: Sedimentological analyses of Martian gullies: the
559 subsurface as the key to the surface, Icarus, 258, 92–108, doi: https://doi.org/10.1016/j.icarus.2015.06.017, 2015a.

560 de Haas, T., Kleinhans, M. G., Carbonneau, P. E., Rubensdotter, L., & Hauber, E.: Surface morphology of fans in the high-
561 Arctic periglacial environment of Svalbard: Controls and processes, Earth-Science Reviews, 146, 163-182, doi:
562 https://doi.org/10.1016/j.earscirev.2015.04.004, 2015b.

563 de Scally, F. A., & Owens, I. F.: Morphometric controls and geomorphic responses on fans in the Southern Alps, New Zealand,
564 Earth Surface Processes and Landforms: The Journal of the British Geomorphological Research Group, 29(3), 311-322, doi:
565 https://doi.org/10.1002/esp.1022, 2004.

566 De Scally, F.A., Owens, I.F., Louis, J.: Controls on fan depositional processes in the schist ranges of the Southern Alps, New
567 Zealand, and implications for debris-flow hazard assessment, Geomorphology 122 (1–2), 99–116, doi:
568 https://doi.org/10.1016/j.geomorph.2010.06.002, 2010.

569 Dickson, J.L. & Head, J.W.: The formation and evolution of youthful gullies on Mars: gullies as the latestage phase of Mars
570 most recent ice age, Icarus, 204, 63–86, doi: https://doi.org/10.1016/j.icarus.2009.06.018, 2009.

571 Dickson, J.L. et al.: Recent climate cycles on Mars: Stratigraphic relationships between multiple generations of gullies and the
572 latitude dependent mantle, Icarus 252, 83–94, doi: http://dx.doi.org/10.1016/j.icarus.2014.12.035, 2015.

573 Dickson, J.L., Head, J.W., Fassett, C.I.: Patterns of accumulation and flow of ice in the mid-latitudes of Mars during the
574 Amazonian, Icarus 219, 723–732, doi: http://dx.doi.org/10.1016/j.icarus.2012.03.010, 2012.

575 Dickson, J.L., Head, J.W., Kreslavsky, M.: Martian gullies in the southern midlatitudes of Mars: Evidence for climate-
576 controlled formation of young fluvial features based upon local and global topography, Icarus 188, 315–323, doi:
577 https://doi.org/10.1016/j.icarus.2006.11.020, 2007.

578 Dundas, C. M., McEwen, A. S., Diniega, S., Hansen, C. J., Byrne, S., & McElwaine, J. N.: The formation of gullies on Mars
579 today, Geol. Soc. Lond. Spec. Publ. 467, 67-94, doi: https://doi.org/10.1144/SP46, 2019.

580 Dundas, C.M., Diniega, S., Hansen, C.J., Byrne, S., McEwen, A.S.: Seasonal activity and morphological changes in martian
581 gullies, Icarus 220:124–143, doi: https://doi.org/10.1016/j.icarus.2012.04.005, 2012.

582 Dundas, C.M., Diniega, S., McEwen, A.S.: Long-term monitoring of Martian gully formation and evolution with
583 MRO/HiRISE, Icarus 251:244–263, doi: https://doi.org/10.1016/j.icarus.2014.05.013, 2015.

584 Hargitai, H. (2014). Viscous Flow Features (Mars). In: Encyclopedia of Planetary Landforms. Springer, New York, NY.
585 https://doi.org/10.1007/978-1-4614-9213-9_596-1

586 Harrison, T.N., Osinski, G.R., Tornabene, L.L., Jones, E.: Global documentation of gullies with the Mars reconnaissance
587 orbiter context camera and implications for their formation, Icarus 252:236–254, doi:
588 https://doi.org/10.1016/j.icarus.2015.01.022, 2015.

589 Hartley, A.J., Mather, A.E., Jolley, E., Turner, P.: Climatic controls on alluvial-fan activity, Coastal Cordillera, northern Chile.
590 In: Harvey, A.M., Mather, A.E., Stokes, M. (Eds.), Alluvial Fans: Geomorphology, Sedimentology, Dynamics. Geol. Soc.
591 Lond. Spec. Publ. 251, 95-115, doi: https://doi.org/10.1144/GSL.SP.2005.251.01., 2005.

592 Head, J.W., Marchant, D.R., Dickson, J.L., Kress, A.M., Baker, D.M.: Northern midlatitude glaciation in the Late Amazonian
593 period of Mars: criteria for the recognition of debris-covered glacier and valley glacier landsystem deposits, Earth Planet. Sci.
594 Lett. 294:306–320, doi: https://doi.org/10.1016/j.epsl.2009.06.041, 2010.

595 HELDMANN, J.L. & MELLON, M.T.: Observations of Martian gullies and constraints on potential formation mechanisms,
596 Icarus, 168, 285–304, doi: https://doi.org/10.1016/j.icarus.2003.11.024, 2004.

597 Heldmann, J.L. et al.: Formation of martian gullies by the action of liquid water flowing under current martian environmental
598 conditions, J. Geophys. Res. Planets 110, doi: http://dx.doi.org/10.1029/2004JE002261, 2005.

599 Hobbs, S.W., Paull, D.J., Clark, J.D.A.: A comparison of semiarid and subhumid terrestrial gullies with gullies on Mars:
600 Implications for martian gully erosion, Geomorphology 204, 344–365, doi: http://dx.doi.org/10.1016/j.geomorph.2013.08.018,
601 2014.

602 Hobbs, S.W., Paull, D.J. and Clarke, J.D.A.: Analysis of regional gullies within Noachis Terra, Mars: A complex relationship
603 between slope, surface material and aspect, Icarus, 250, 308-331, doi: https://doi.org/10.1016/j.icarus.2014.12.011, 2015.

Hubbard, B., Milliken, R.E., Kargel, J.S., Limaye, A. & Souness, C.: Geomorphological characterisation and interpretation of a mid-latitude glacier-like form: Hellas Planitia, Mars, Icarus, 211, 330–346, doi: https://doi.org/10.1016/j.icarus.2010.10.021, 2011.

Ilinca, V.: Using morphometrics to distinguish between debris flow, debris flood and flood (Southern Carpathians, Romania), Catena, 197, 104982, doi: https://doi.org/10.1016/j.catena.2020.104982, 2021.

Jackson LE, Kostaschuk RA, MacDonald GM: Identification of debris flow hazard on alluvial fans in the Canadian Rocky Mountains, In: Costa JE, Wieczorek GF (eds) Debris flows/avalanches: process, recognition, and mitigation. Rev Eng Geol vol. VII. Geol. Soc. Am, doi: https://doi.org/10.1130/REG7-p115, 1987.

Johnsson, A. et al.: Evidence for very recent melt-water and debris flow activity in gullies in a young mid-latitude crater on Mars, Icarus 235, 37–54, doi: http://dx.doi.org/10.1016/j.icarus.2014.03.005, 2014.

Kirk, R.L., Howington-Kraus, E., Rosiek, M.R., Anderson, J.A., Archinal, B.A., Becker, K.J., Cook, D.A., Galuszka, D.M., Geissler, P.E., Hare, T.M., Holmberg, I.M., Keszthelyi, L.P., Redding, B.L., Delamere, W.A., Gallagher, D., Chapel, J.D., Eliason, E.M., King, R., McEwen, A.S.: Ultrahigh resolution topographic mapping of Mars with MRO HiRISE stereo images: meter-scale slopes of candidate Phoenix landing sites, J. Geophys. Res. Planets 113, doi: https://doi.org/10.1029/2007JE003000, 2008.

Kostaschuk, R.A., Macdonald, G.M., Putnam, P.E.: Depositional process and alluvial fan-drainage basin morphometric relationships near banff, Alberta, Canada, Earth Surf. Proc. Land. 11 (5), 471–484, doi: https://doi.org/10.1002/esp.3290110502, 1986.

Kreslavsky, M.A.: Slope steepness of channels and aprons: Implications for origin of martian gullies. Workshop Martian Gullies, Workshop on Martian Gullies 2008. Abs.#1301, 2008.

Kreslavsky, M.A., Head, J.W.: Mars: nature and evolution of young latitudedependent water-ice-rich mantle, Geophys. Res. Lett. 29, doi: https://doi.org/10.1029/2002GL015392, 2002.

Langbein, W. B.: Profiles of rivers of uniform discharge, U.S. Geol. Surv. Prof. Pap., 501-B, 119– 122, doi: https://doi.org/10.1086/627653, 1964.

Lanza, N. L., Meyer, G. A., Okubo, C. H., Newsom, H. E., & Wiens, R. C.: Evidence for debris flow gully formation initiated by shallow subsurface water on Mars, Icarus, 205(1), 103-112, doi: https://doi.org/10.1016/j.icarus.2009.04.014, 2010.

Levy, J.S. et al.: Identification of gully debris flow deposits in Protonilus Mensae, Mars: Characterization of a water-bearing, energetic gully-forming process, Earth Planet. Sci. Lett. Mars Express after 6 Years in Orbit: Mars Geology from Three-Dimensional Mapping by the High Resolution Stereo Camera (HRSC) Experiment 294, 368–377, doi: https://doi.org/10.1016/j.epsl.2009.08.002, 2010b.

Levy, J.S., Head, J., Marchant, D.: Thermal contraction crack polygons on Mars: classification, distribution, and climate implications from HiRISE observations, J. Geophys.Res. Planets 114, 01007, doi: https://doi.org/10.1029/2008JE003273, 2009a.

Levy, J. S., Head, J. W., Marchant, D. R., Dickson, J. L., & Morgan, G. A.: Geologically recent gully–polygon relationships on Mars: Insights from the Antarctic Dry Valleys on the roles of permafrost, microclimates, and water sources for surface flow, Icarus, 201(1), 113-126, doi: https://doi.org/10.1016/j.icarus.2008.12.043, 2009b.

Levy, J.S., Head, J.W., Marchant, D.R.: Gullies, polygons and mantles in Martian permafrost environments: cold desert landforms and sedimentary processes during recent Martian geological history, Geol. Soc. Lond. Spec. Publ. 354, 167–182, doi: https://doi.org/10.1144/SP354.10, 2011.

Malin, M.C., Edgett, K.S.: Evidence for recent groundwater seepage and surface runoff on Mars. Science 288:2330–2335, doi: https://doi.org/10.1126/science.288.5475.2330, 2000.

Mcewen, A.S., Eliason, E.M. et al.: Mars reconnaissance orbiter's High Resolution Imaging Science Experiment (HiRISE), J. Geophys. Res.: Planets, 112, E05S02, doi: https://doi.org/10.1029/2005JE002605, 2007.

McLachlan, G. J.: Discriminant analysis and statistical pattern recognition, John Wiley & Sons, 2005.

Melton, M.A.: An analysis of the relation among elements of climate, surface properties and geomorphology, Office of Nav. Res. Dept. Geol. Columbia Univ, NY. Tech. Rep. 11, 1975.

Milliken, R.E., Mustard, J.F., Goldsby, D.L.: Viscous flow features on the surface of Mars: observations from high-resolution Mars Orbiter Camera (MOC) images, J. Geophys. Res. 108, doi: https://doi.org/10.1029/2002JE002005, 2003.

Mustard, J.F., Cooper, C.D., Rifkin, M.K.: Evidence for recent climate change on Mars from the identification of youthful near-surface ground ice, Nature 412:411–414, doi: https://doi.org/10.1038/35086515, 2001.

Phillips, J.D., Lutz, J.D.: Profile convexities in bedrock and alluvial streams, Geomorphology 102, 554–566, doi: https://doi.org/10.1016/j.geomorph.2008.05.042, 2008.

Pilorget, C. & Forget: Formation of gullies on mars by debris flows triggered by CO2 sublimation, Nature Geoscience, 9, 65–69, doi: https://doi.org/10.1038/ngeo2619, 2016.

Plaut, Jeffrey J., Ali Safaeinili, John W. Holt, Roger J. Phillips, James W. Head III, Roberto Seu, Nathaniel E. Putzig, and Alessandro Frigeri: Radar evidence for ice in lobate debris aprons in the mid-northern latitudes of Mars, Geophysical research letters 36, no. 2, doi: https://doi.org/10.1029/2008GL036379.

Reiss, D. et al.: Absolute dune ages and implications for the time of formation of gullies in Nirgal Vallis, Mars. J. Geophys. Res.-Planets 109, doi: http://dx.doi.org/10.1029/2004JE002251, 2004.

663 Reiss, D., Hauber, E. et al.: Terrestrial gullies and debris-flow tracks on Svalbard as planetary analogs for Mars, In: Garry,
664 W.B. & Bleacher, J.E. (eds) Analogs for Planetary Exploration, Geol. Soc. Am. Spec. Papers 483, 165–175, doi:
665 https://doi.org/10.1130/2011.2483(11), 2011.

666 Rodine, J.D., Johnson, A.M.: The ability of debris, heavily freighted with coarse clastic materials, to flow on gentle slopes,
667 Sedimentology 23, 213–234, doi: https://doi.org/10.1111/j.1365-3091.1976.tb00047.x, 1976.

668 Ryder, J.: Some aspects of the morphometry of paraglacial alluvial fans in South-central British Columbia, Canadian Journal
669 of Earth Sciences 8: 1252-1264, doi: https://doi.org/10.1139/e71-11, 1971.

670 Schon, S.C., Head, J.W., Fassett, C.I.: Unique chronostratigraphic marker in depositional fan stratigraphy on Mars: Evidence
671 for ca. 1.25 Ma gully activity and surficial meltwater origin, Geology 37, 207–210, doi: http://dx.doi.org/10.1130/g25398a.1,
672 2009.

673 Siewert, M. B., Krautblatter, M., Christiansen, H. H., & Eckerstorfer, M.: Arctic rockwall retreat rates estimated using
674 laboratory-calibrated ERT measurements of talus cones in Longyeardalen, Svalbard, Earth Surface Processes and Landforms,
675 37(14), 1542-1555, doi: https://doi.org/10.1002/esp.3297, 2012.

676 Sinha, R. K., Ray, D., De Haas, T., & Conway, S. J.: Global documentation of overlapping lobate deposits in Martian gullies.
677 Icarus, 352, 113979, doi: https://doi.org/10.1016/j.icarus.2020.113979, 2020.

678 Sinha, R. K., Vijayan, S., Shukla, A. D., Das, P., & Bhattacharya, F.: Gullies and debris-flows in Ladakh Himalaya, India: a
679 potential Martian analogue, Geol. Soc. Lond. Spec. Publ. 467, 315-342, doi: https://doi.org/10.1144/SP46, 2019.

680 Sinha, R.K., Vijayan, S.: Geomorphic investigation of craters in Alba Mons, Mars: implications for Late Amazonian glacial
681 activity in the region, Planet. Space Sci. 144:32–48, doi: https://doi.org/10.1016/j.pss.2017.05.014, 2017.

682 Souness, C., & Hubbard, B.: Mid-latitude glaciation on Mars, Progress in Physical Geography, 36(2), 238-261, doi:
683 https://doi.org/10.1177/030913331243, 2012.

684 Souness, C., Hubbard, B., Milliken, R. E., & Quincey, D.: An inventory and population-scale analysis of martian glacier-like
685 forms, Icarus, 217(1), 243-255, doi: https://doi.org/10.1016/j.icarus.2011.10.020, 2012.

686 Stock, J.D., Dietrich, W.E.: Erosion of steepland valleys by debris flow, Geol. Soc. Am. Bull. 118 (9/10), 1125–1148.
687 doi:10.1130/B25902.1, 2006.

688 Stolle, A., Langer, M., Blöthe, J. H., & Korup, O.: On predicting debris flows in arid mountain belts, Global and Planetary
689 Change, 126, 1-13, doi: https://doi.org/10.1016/j.gloplacha.2014.12.005, 2015.

690 Welsh, A., Davies, T.: Identification of alluvial fans susceptible to debris-flow hazards. Landslides 8 (2), 183–194, doi:
691 https://doi.org/10.1007/s10346-010-0238-4, 2011.

Wilford, D. J., Sakals, M. E., Innes, J. L., Sidle, R. C., & Bergerud, W. A.: Recognition of debris flow, debris flood and flood hazard through watershed morphometrics, Landslides, 1(1), 61-66, doi: https://doi.org/10.1007/s10346-003-0002-0, 2004.

Yue, Z., Hu, W., Liu, B., Liu, Y., Sun, X., Zhao, Q. and Di, K.: Quantitative analysis of the morphology of martian gullies and insights into their formation, Icarus, 243, pp.208-221, doi: https://doi.org/10.1016/j.icarus.2014.08.028, 2014.